Invited - Terahertz Quantum Cascade Lasers

Giles Davies[1] and Edmund Linfield[2]

[1]School of Electronic and Electrical Engineering, University of Leeds, Leeds LS2 9JT, UK

[2]Cavendish Laboratory, University of Cambridge, Madingley Road, Cambridge CB3 0HE, UK

ABSTRACT — **Quantum cascade lasers operating at far-infrared (terahertz) frequencies have now been demonstrated. We review the fabrication, operation, and performance of these lasers, and indicate recent results in which devices have been developed to operate continuous wave, at temperatures greater than 77 K, emit at frequencies down to 3.5 THz, and produce tens of milli-Watts of power. These results are an encouraging step towards a widely applicable solid-state terahertz source, and the development of terahertz photonics.**

I. INTRODUCTION

The terahertz (THz) frequency range, lying between microwave and mid-infrared frequencies (Fig. 1), represents a significant portion of the electromagnetic spectrum for which compact, solid-state sources that operate at room temperature are not available. On the microwave side of this range, it is difficult to fabricate electronic devices that operate at frequencies substantially above a few hundred GHz [1] (although the output of such sources can be harmonically multiplied to the THz range [2]). This is partially a result of the inherent need for very short carrier transit times in the active regions and is also a consequence of only low powers being delivered by devices which must have small device areas to minimise the device capacitance. On the optical side, the lack of suitable semiconductors prevents the extension into the far-infrared of the interband diode laser concept, which is exploited for operation at visible and near-infrared frequencies.

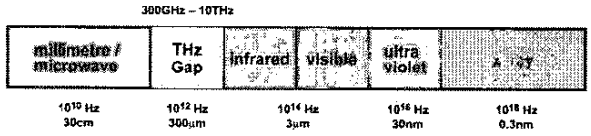

Fig. 1. A schematic representation of the electromagnetic spectrum showing the THz region.

THz radiation, however, can be generated in solid-state sources by mixing two visible laser beams in a suitable photomixer [3], the transient acceleration of charges generated by femtosecond near-infrared/visible pulses [4], the silicon-impurity laser [5], and the *p*-doped germanium laser [6]. Each of these techniques, however, lacks compactness, integrability and portability, as well as suffering, for example, from low output powers, limited tunability, or the need for liquid helium cryogenics.

Nevertheless, such sources have demonstrated that THz radiation has considerable potential for a wide range of sensing, imaging, and spectroscopy measurements. Examples include: non-contact, label-free probing of genes [7]; the investigation of many-particle interactions in electron-hole plasmas [8]; the identification of skin cancers [9]; together with many other applications across the physical, medical, and biological sciences.

II. THE QUANTUM CASCADE LASER

Recent research into solid-state THz sources has made extensive use of the quantum cascade laser (QCL) concept. A QCL is a layered semiconductor device comprising a series of coupled quantum wells which can be grown by molecular beam epitaxy (MBE). By appropriately engineering the thickness and composition of the sequentially grown epitaxial layers, the conduction band is split by quantum confinement into a number of discrete electronic subbands. The corresponding inter-subband electron transition energies, under an appropriate applied electric field, can in principle be tailored to cover a wide range of wavelengths from the far- to the mid-infrared. These unipolar injection lasers, are named 'quantum cascade' from the possibility of stacking together successive active regions to generate many photons for each injected electron. Originally established in the mid-infrared [10], QCLs have been now demonstrated at room temperature up to a longest wavelength of 24 μm (12.5 THz) [11].

Although the original mid-infrared QCL design employed inter-subband transitions, the adoption of superlattice active regions with the electrons transported though minibands, conferred the advantage of large current densities (and hence large optical powers) with reduced level misalignment. Inter-miniband lasing takes place between states at the edges of the first minigap, with the relatively long inter-miniband relaxation time (in comparison with the intra-miniband time) working in favour of the design [12,13]. At the same time, a large dipole matrix element is ensured by the minibands being uniformly delocalised over a number of semiconductor layers. Electrons extracted

0-7803-7695-1/03/$17.00 © 2003 IEEE

from the lowest miniband of one superlattice are injected into the second miniband of the next superlattice.

A problem, however, was how to maintain a flat superlattice band profile under an applied bias. The active regions can be doped, but this results in higher optical losses, broad emission linewidths, and reduced population inversion at high temperatures. Thus, although these lasers were capable of higher output powers, they had larger threshold current densities than standard QCLs of the same wavelength, impeding room temperature or continuous wave (CW) operation [12].

Tredicucci *et al.* addressed this problem with a design in which the doping was placed in suitably designed injector regions which exactly compensated the applied electric field over the active superlattices [12]. This produced flat minibands, efficient injection between subsequent cascade units, and reduced impurity scattering. Threshold currents resulted which were a factor of two lower than had been previously achieved, and room temperature operation at 7 μm was observed.

Tredicucci *et al.* subsequently proposed a further design in which flat minibands were obtained under an applied operating bias by subtly engineering the width of each superlattice layer [13]. Such 'chirped' superlattices had undoped active regions and lower doping in the injector regions than in the previous design, and led to record peak emission powers at 7.6μm at room temperature, with the lowest reported QCL threshold current density at the time.

More recently, Faist *et al.* adopted a design that can be thought of as a hybrid between the original QCL intersubband structure and the superlattice scheme discussed above [14]. The active region again comprises a chirped superlattice, but there is no distinct injector region, and the upper lasing level is a single electronic subband extending into the first minigap. The rational behind this design is to combine a high upper level injection efficiency (obtained by resonant tunnelling), with a high lower level extraction efficiency (via the miniband). These 9.1 μm 'bound-to-continuum' structures showed low threshold current densities and excellent high temperature operation [14].

III. The Extension to the Far-Infrared

It was originally believed that it would be easier to realize an intersubband QCL in the far-infrared rather than in the mid-infrared, because once the laser transition energy is smaller than the optical phonon energy, a competing depopulation mechanism of the upper lasing level is eliminated. In fact, optical phonon emission proved to play a significant role in electron cooling in mid-infrared QCLs, and many designs exploited resonant optical phonon emission to reduce the lower lasing level lifetime [15,16].

There are many challenges in extending the QCL concept to the far-infrared: for example, free carrier absorption in semiconductors scales approximately as the wavelength squared requiring a large-gain active region, and the small energy (10–20 meV) of the optical transition necessitates very selective injection. Furthermore, there are difficulties in waveguiding THz radiation in an active material that is just a few microns thick. A conventional dielectric waveguide using semiconductor cladding layers of smaller refractive index would not only require prohibitive thicknesses for MBE growth but would also result in small confinement factors.

Despite these issues, THz QCLs have recently been demonstrated, although operation is confined to cryogenic temperatures at present, and we next discuss the first working THz QCL in detail.

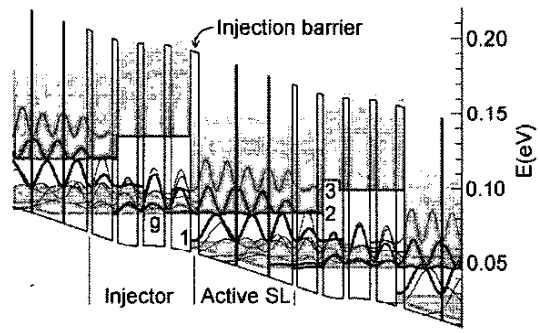

Fig. 2. Conduction band structure of a 67 μm chirped superlattice quantum cascade emitter (from Ref. 17).

IV. THz Quantum Cascade Lasers

A self-consistent calculation of the conduction band of the first THz QCL, realized by Köhler *et al.* [17], is shown in Fig. 2. The structure comprises a three GaAs-$Al_{0.15}Ga_{0.85}As$ quantum well chirped active superlattice (SL), alternating with a four quantum well injector [18, 19]; the figure shows two of the 104 periods grown, under an electric field of 3.5 kV/cm. The layer thicknesses, in nm, starting from the injection barrier are ***4.3/ 18.8/ 0.8/ 15.8/ 0.6/ 11.7/ 2.5/*** 10.3/ **2.9**/ 10.2/ **3.0**/ 10.8/ **3.3**/ 9.9, where $Al_{0.15}Ga_{0.85}As$ layers are in bold face, the active region is in italic, and the 10.2-nm-wide well is silicon-doped at 4×10^{16} cm^{-3}. The moduli squared of the wavefunctions are also shown in Fig. 2, together with the miniband regions (shaded).

The optical transition takes place across the 18-meV-wide (67 μm, 4.4 TIIz) minigap between the second and first minibands (states *2* and *1*) and, being vertical in real space, presents a large dipole matrix element of 7.8 nm. Carriers are injected into state *2* via resonant tunnelling from the injector ground state labeled *g*. The lower laser

state *1* is strongly coupled to a wide injector miniband, comprising seven subbands spanning 17 meV. This provides a large phase space where electrons scattered either from subband *2* or directly from the injector can spread, at the same time ensuring fast depletion of state *1*. Moreover, the wide miniband allows efficient electrical transport, even at high current densities, and simultaneously suppresses thermal backfilling. This design was supported by theoretical modeling employing a Monte-Carlo scheme based on a coupled set of three-dimensional Boltzmann equations [20], including all relevant energy-relaxation mechanisms, such as carrier-carrier and carrier-LO-phonon scattering processes [21].

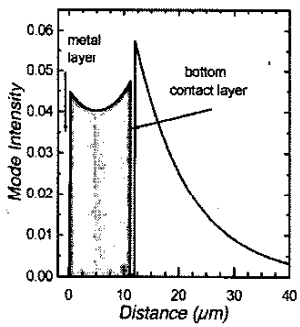

Fig. 3. Vertical profile through quantum cascade structure, showing optical confinement in waveguide (from Ref. 17).

Following demonstration of the predicted electroluminescence from this structure [19], consideration was given to an appropriate waveguide – a crucial part of any working THz QCL design [22]. At THz frequencies, a simple single surface-plasmon waveguide results in a small overlap of the optical mode with any active region of reasonable thickness. Therefore, a thin (800 nm) n^+ GaAs layer was grown on top of the undoped GaAs substrate, below the active superlattice, to create a strongly confined, low loss *TM* mode bound to that layer (and was additionally used for electrical contacting). A silicon donor density of 2×10^{18} cm^{-3} provided a good compromise between absorption losses and overlap with the active region. Above the active region, a 200-nm-thick GaAs layer doped to 5×10^{18} cm^{-3} together with its metallic contact led to the mode profile in Fig. 3. A comparison between different waveguide schemes has been made for a similar THz QCL design by Rochat *et al.* [16].

The wafer was processed into mesa-etched ridge stripes, thinned to about 200 μm to improve heat dissipation, and Ge/Au ohmic contacts deposited. A Fabry-Perot cavity was then formed by cleaving the stripes into laser bars. The facets were left uncoated in this study, although the adoption of a high-reflectivity back facet coating proves advantageous [16]. The devices were mounted onto the cold finger of a liquid-helium cryostat and current pulses were applied to avoid excess heating in the device. The emitted radiation was passed through a Fourier transform interferometer (FTIR), and focused onto a liquid-helium-cooled silicon bolometer. The beam path was purged with purified air to minimize water-vapour absorption. Sub-threshold spectra were recorded using the FTIR in step-scan mode, employing a lock-in amplifier for signal detection. Lasing spectra were collected in rapid scan mode with a DTGS (deuterated triglycine sulfate) detector.

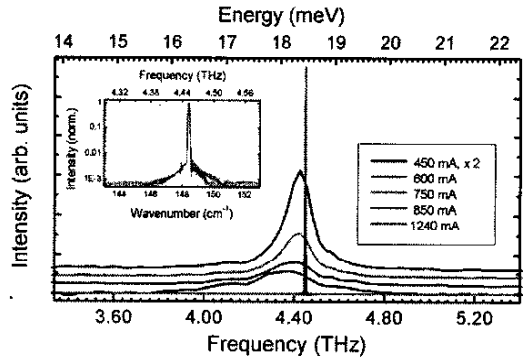

Fig. 4. Emission from 67 μm chirped superlattice quantum cascade emitter (from Ref. 17).

Fig. 4 shows the emission spectra of a 1.2-mm-long, 180-μm-wide laser for different drive currents at 8 K. The characteristic narrowing of the emission line, and nonlinear dependence of the intensity, are clearly observed up to around 880 mA, where laser threshold is reached. Lasing takes place at 4.4 THz (67 μm), on the high-energy side of the luminescence line, probably owing to the reduced waveguide losses at shorter wavelengths.

The output peak power was estimated to be 2 mW at a heat-sink temperature of 5 K, with a threshold current density and electric field of 390 A/cm^2 and 5.5 kV/cm, respectively. The maximum operating temperature was 45 K. Single-mode emission was obtained, most likely a consequence of the relatively narrow gain spectrum and the wide Fabry-Perot mode spacing. The linewidth is limited by the resolution of the spectrometer (3.75 GHz) (Fig. 4 inset). The spontaneous emission at low drive currents (300 mA) displays a full width at half-maximum of 2 meV, similar to that obtained from luminescence structures with only 40 periods [19]. These latter spectra are best fitted with a Lorentzian, which, together with the absence of any broadening when increasing the number of periods, indicates the high growth quality and uniformity throughout the whole 10-μm-thick active material stack – a critical feature in realizing working THz QCLs.

VI. Recent Developments

For many practical applications, CW operation is advantageous. This has been achieved recently through improvements in the laser device fabrication (facet coating, reduction in parasitic resistances, and improved thermal management), together with optimization of device dimensions. Combined, these have led to lower threshold currents and reduced heating [23–25]. CW output powers of several milli-Watts have been reported for 67 μm wavelength devices at liquid helium temperatures, with CW operation maintained up to around 50 K [24].

It is also important to be able to produce a QCL with an emission frequency tailored appropriately for the relevant application. Following the chirped superlattice approach, Köhler *et al.* have demonstrated CW operation at 3.5 THz (85 μm) [26]. Other active layer designs are also being investigated, paralleling previous work in the mid-infrared. Williams *et al.* have adopted a fast optical phonon depopulation scheme of the lower lasing level in their 3.4 THz QCL design [27]. Furthermore, Scalari *et al.* have employed a bound-to-continuum design to achieve emission at 3.5 THz with a record high operating temperature of 90 K [28].

These are important advances for the widespread use of THz QCLs, and the development of terahertz photonics.

Acknowledgement

The authors are grateful for the help and support of A Tredicucci, R Köhler, F Beltram, R C Iotti, F Rossi, J Faist, M Rochat, G Scalari, L Ajili, H Willenberg, H E Beere, D A Ritchie, D D Arnone, S S Dhillon, S Barbieri, J Alton, C Sirtori, and M Pepper. Most of the THz QCL research reported in this paper was supported in part by the European Commission through the IST Framework V FET project *WANTED*. AGD and EHL acknowledge the financial support of the Royal Society and Toshiba Research Europe Limited, respectively.

References

[1] see, for example, J. M. Chamberlain, R. E. Miles, C. E. Collins, D. P. Steenson in 'New Directions in Terahertz Technology', eds J. M. Chamberlain and R. E. Miles (NATO ASI series, Kluwer, 1997), and references therein.

[2] T. W. Crowe, T. C. Grein, R. Zimmerman, P. Zimmerman, IEEE Microwave and Guided Wave Lett. 6, 207–208 (1996); H. Eisele, A. Rydberg, G. I. Haddad, IEEE Trans. Microwave Theory and Techs. 48, 626–631 (2000).

[3] E. R. Brown, K. A. McIntosh, K. B. Nichols, C. L. Dennis, Appl. Phys. Lett. 66, 285 (1995).

[4] D. H. Auston, Appl. Phys. Lett. 26, 101–103 (1975); A. G Davies, E. H. Linfield, M. B. Johnston, Phys. Med. Biol. 47, 3679–3689 (2002), and references therein.

[5] S. G. Pavlov *et al.*, Appl. Phys Lett. 80, 4717 (2002), and references therein.

[6] E. Bründermann, D. R. Chamberlain, E. E. Haller, Appl. Phys. Lett. 76, 2991–2993 (2000).

[7] P. Bolivar, M. Brucherseifer, M. Nagel, H. Kurz, A. Bosserhoff, R. Büttner, Phys. Med. Biol. 47, 3815–3821 (2002).

[8] R. Huber, F. Tauser, A. Brodschelm, M. Bichler, G. Abstreiter, A. Leitenstorfer, Nature (London) 414, 286–289, 15 November 2001.

[9] R. M. Woodward, B. E. Cole, V. P. Wallace, R. J. Pye, D. D. Arnone, E. H. Linfield, M. Pepper, Phys. Med. Biol. 47, 3853–3863 (2002).

[10] J. Faist, F. Capasso, D. L. Sivco, C. Sirtori, A. L. Hutchinson, A. Y. Cho, Science 264, 553–556 (1994).

[11] R. Colombelli, F. Capasso, C. Gmachl, A. L. Hutchinson, D. L. Sivco, A. Tredicucci, M. C. Wanke, A. M. Sergent, A. Y. Cho, Appl. Phys. Lett. 78, 2620–2622 (2001).

[12] A. Tredicucci, F. Capasso, C. Grachl, D. L. Sivco, A. L. Hutchinson, A. Y. Cho, J. Faist, G. Scamarcio, Appl. Phys. Lett. 72, 2388–2390 (1998).

[13] A. Tredicucci, F. Capasso, C. Grachl, D. L. Sivco, A. L. Hutchinson, A. Y. Cho, Appl. Phys. Lett. 73, 2101–2103 (1998).

[14] J. Faist, M. Beck, T. Aellen, E. Gini, Appl. Phys. Lett. 78, 147–149 (2001).

[15] M. Rochat, J. Faist, M. Beck, U. Oesterle, M. Ilegems, Appl. Phys. Lett. 73, 3724–3726 (1998).

[16] M. Rochat, L. Ajili, H. Willenberg, J. Faist, H. Beere, G. Davies, E. Linfield, D. Ritchie, Appl. Phys. Lett. 81, 1381–1383 (2002).

[17] R. Köhler, A. Tredicucci, F. Beltram, H. E. Beere, E. H. Linfield, A. G. Davies, D. A. Ritchie, R. C. Iotti, F. Rossi, Nature (London) 417, 156–159, 9 May 2002.

[18] R. Köhler, R. C. Iotti, A. Tredicucci, F. Rossi, Appl. Phys. Lett. 79, 3920–3922 (2001).

[19] R. Köhler, A. Tredicucci, F. Beltram, H. E. Beere, E. H. Linfield, A. G. Davies, D. A. Ritchie, Appl. Phys. Lett. 80, 1867–1869 (2002).

[20] R. C. Iotti and F. Rossi, Phys. Rev. Lett. 87, article 146603 (2001).

[21] R. C. Iotti and F. Rossi, App. Phys. Lett., 78, 2902–2904 (2001).

[22] M. Rochat, M. Beck, J. Faist, U. Oesterle, Appl. Phys. Lett. 78, 1967–1969 (2001).

[23] L. Ajili, G. Scalari, H. Willenberg, D. Hofstetter, M. Beck, J. Faist, H. E. Beere, A. G. Davies, E. H. Linfield, D. A. Ritchie, Electronics Lett. 38, 1675–1676 (2002).

[24] R. Köhler, A. Tredicucci, F. Beltram, H. E. Beere, E. H. Linfield, A. G. Davies, D. A. Ritchie, S. S. Dhillon, C. Sirtori, Appl. Phys. Lett. 82, 1518–1520 (2003).

[25] S. Barbieri, J. Alton, M. Evans, S. S. Dhillon, H. E. Beere, E. H. Linfield, A. G. Davies, D. A. Ritchie, R. Köhler, A. Tredicucci, F. Beltram, IEEE Journal of Quantum Electronics (2003), in the press.

[26] R. Köhler, A. Tredicucci, F. Beltram, H. E. Beere, E. H. Linfield, A. G. Davies, D. Ritchie, Optics Lett. (2003), in press.

[27] B. S. Williams, H. Callebaut, S. Kumar, Q. Hu, J. L. Reno, Appl. Phys. Lett. 82, 1015–1017 (2003).

[28] G. Scalari and J. Faist, private communication.